High-resolution extreme-ultraviolet spectrum of He between 35 and 55 eV

P. Baltzer and L. Karlsson
Department of Physics, University of Uppsala, Box 530, S-751 21 Uppsala, Sweden
(Received 1 February 1988)

The photon emission spectrum from He between 35 and 55 eV has been studied by means of a 3-m normal-incidence grating spectrometer. The radiation was generated by a new vuv-microwave source employing cyclotron resonance obtained by a static magnetic field. A large number of lines have been observed in the spectrum. Many Rydberg series have been identified not only for singly excited atoms but also for doubly excited atoms. The series involve both singlet and triplet states. The energy of many doubly excited states have been determined more accurately than in previous studies and in addition some new energies have been measured. The lines observed correspond to both one-electron and two-electron transitions, indicating that configuration interaction is important.

I. INTRODUCTION

The radiative transitions of the helium atom and positive ion have been studied extensively. As a result, the term scheme is in many parts very well established. In particular this applies to the single-electron excitations but many studies have also been performed to determine doubly excited states of He I. Experimental data obtained in studies before 1973 are collected in Ref. 1. Later results can be found in Refs. 2–8.

The doubly excited states all lie above the ionization limit for He I (at 24.5876 eV). They are therefore energetically susceptible to autoionization and produce in many cases practically no radiation. However, due to symmetry restrictions autoionization is inhibited for certain states and in such cases radiative transitions can give rise to sharp lines in spectra. This applies to the doubly excited states $^{1,3}P^e$, $^{1,3}D^o$, and $^{1,3}F^e$, which in the LS-coupling approximation cannot interact with the ionization continuum below the $n=2$ limit of He II. In other cases the autoionization rate in allowed transitions into the ionization continuum can be sufficiently low for sharp lines to appear in the photon emission. An intermediate situation where the emission line is considerably lifetime broadened by autoionization is observed in this study for the $2s2p\ ^3P \rightarrow 1s2s\ ^3S$ transition.

The present investigation has been performed on radiation emitted from a uv line source originally designed for uv photoelectron spectroscopy. This source provides a very intense photon flux by means of a microwave discharge in a low pressure gas. By applying a strong, inhomogeneous magnetic field in the discharge region cyclotron resonance is obtained which increases the total intensity substantially and allows the discharge to be maintained at very low pressures. The resonance lines produced under such conditions are narrow, and furthermore, a wealth of lines are generated. This new uv source will be described in a separate publication.[9]

By studying the uv radiation from He in a 3-m normal-incidence grating spectrometer we have been able to observe a large number of lines. In particular, many of these lines can be readily identified as components of Rydberg series in doubly excited He I. Previous studies have mostly been performed by means of beam-foil spectroscopy. The resolution in these experiments is usually lower than what can be obtained by the present technique in the energy range studied (the resolution of our instrument is further discussed in Sec. II). The aim of the present study is therefore twofold; one is to demonstrate the usefulness of the new uv source for studies of highly excited states in atoms and the other to provide some additional information on excited states of helium.

II. EXPERIMENTAL DETAILS

The new vuv source, which has been patented in Sweden (publication number 443 062), has the following main novel characteristics. The microwaves are fed into the discharge region through a rectangular waveguide with a cross section of 23 mm $\times$ 10 mm. In the vicinity of the discharge region it is contracted into a ridge structure with outer dimensions of 10 mm $\times$ 10 mm (cf. Fig. 1). Magnet poles are arranged in a way that an inhomogeneous magnetic field is created with lines of force perpendicular to the lines of force from the electric field. A quartz window transparent to the microwave radiation is mounted inside the waveguide to create an air-discharge gas interface. It is placed sufficiently far away from the discharge to remove heat and metallization problems ($\sim$8 cm). The entire waveguide system including the discharge region is made of copper (water cooled) to enhance heat transport. In the region in contact with the plasma the copper surface is lined with tantalum to reduce erosion and subsequent emission of impurity lines and metallization of the window. The idea to use an all-metal system emerged from experiments with microwave-powered discharges in quartz tubes. In these studies it was found that the quartz melted when the microwave power ($\sim$300 W) was applied even without a plasma inside the discharge region. Quartz was chosen since it is the best material with respect to dielectric losses (energy absorption). The new source can run ap-

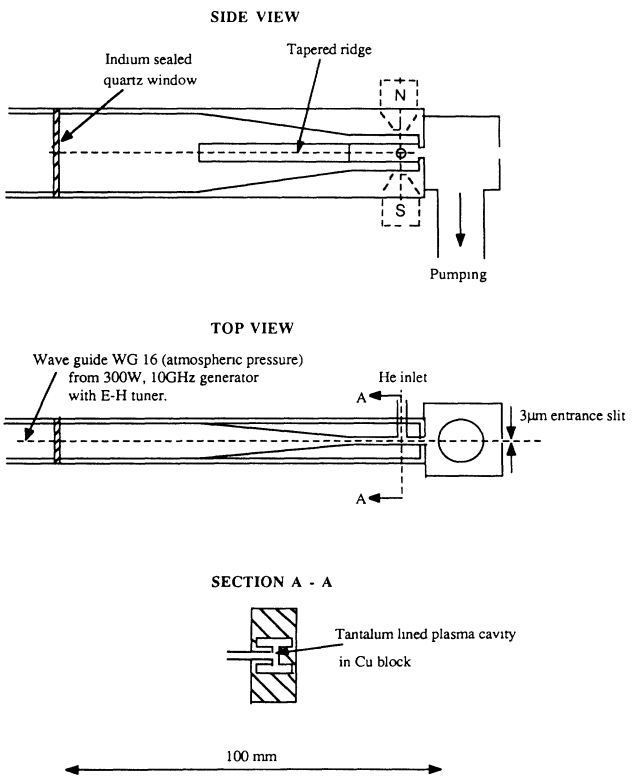

FIG. 1. Scale diagram of the new vuv source.

proximately 500 h on helium before cleaning of the window has to take place.

The magnet configuration gives a field which increases towards the poles, thus providing a magnetic bottle for the electrons. The plasma is powered by a 300-W klystron working at X-band frequencies (10 GHz). The magnetic field corresponding to this frequency has a strength of 0.36 T. This field is produced by a permanent magnet manufactured from a samarium-cobalt alloy, $SmCo_5$. By working under the cyclotron resonance condition, the electrons are efficiently trapped in the magnetic field, and accelerated by the microwave field to high energies, giving high excitation efficiency. Furthermore, since by the tapered ridge configuration of the discharge volume the discharge is highly concentrated in a small region of 2 mm$\times$5 mm$\times$5 mm, the brilliance from the discharge region is very high. Moreover, at these conditions the discharge can be sustained at very low gas pressures (a few millitorr). This reduces the self-absorption of the He I α line very much. The gas pressure used in the present investigation was about 50 mtorr.

The radiation has been studied by means of a 3-m normal-incidence vuv spectrometer (rebuilt Hilger-Watts vacuum spectrograph) using a 50-mm$\times$30-mm reflection grating with 1200 lines/mm. The wavelength range covered in first order operation is 200–1500 Å. Due to the high intensity of our line source it is possible to use a very narrow entrance slit to the spectrometer. In the present studies the slit width was 3 μm as measured by laser diffraction. The resolution in the experiments was therefore determined primarily by the grating. The theoretical resolution is 0.5 meV at 584 Å (the He I α line) whereas in the present experiments a resolution of about 1–2 meV was normally obtained. The final alignment of the grating is made by means of small electric motors mounted on the grating support and running in vacuum. With this arrangement the adjustment can be made easily at any time without breaking vacuum, using a real-time line profile scanner mounted in the plate holder. It incorporates a single narrow slit swept in front of a channel electron multiplier. The design of this device will be presented in a separate publication.[9] All aberrations can be ignored due to the normal incidence. The fact that the observed linewidth is approximately two times the theoretical value is therefore probably due to imperfections in the grating. In most studies photographic plates (Kodak SWR) have been used to record the spectra. The plates were developed in Rodinal 1:25 water solution for 4 min at 20 °C. The unexposed plates were stored at -18 °C. By means of a microdensitometer, specially designed for the purpose, the spectra have been transferred to the form displayed in the figures either by using analog or digital readout. The photometer will be described in a separate publication.[9] Separate lines can also be studied under high resolution by means of the above-mentioned profile scanner. The pressure in the spectrometer was approximately 10^{-5} torr at the recording of the spectra, the gas mainly being He coming from the uv source.

For many lines of the spectrum the wavelength has been determined accurately in previous studies or can be calculated exactly as in the case of the He II lines corresponding to the $np \rightarrow 1s$ transitions. These well-known lines have been used as reference lines for calibration of the spectrum. They include in addition to the He II lines the first components of the $2p^2\,{}^3P \rightarrow 1snp\,{}^3P$ series for which in particular the $2p^2 \rightarrow 1s2p$ line is well determined and in the intermediate wavelength region the two strong lines at 294.11 Å and 311.16 Å. The resulting accuracy in the determination of the wavelength in our spectrum is 0.02 Å for well-defined lines and up to 0.05 Å for weak lines superimposed on stronger components.

III. RESULTS AND DISCUSSION

The spectrum in the range between 350 and 230 Å is dominated by the immense He II α line at 303.78 Å with background scattering tails extending far out on both sides. In addition, numerous comparatively weak lines can be observed superimposed on the tails of the He II α line on a general background of low intensity. Some of these lines correspond to transitions in He II (the $np \rightarrow 1s$ series) but the main part involves transitions from doubly excited states of He I (cf. Figs. 2–5). The dip observed at the intensity maximum of the strongest lines is due to solarization of the plate.

In order to put the large amount of data in legible form we have organized the material in different figures corresponding to certain spectral series and specific details of the spectrum which are not resolved in the overall spectrum. The wavelengths of all assigned and some unassigned lines are given in Table I. The line at 235.42 Å (cf.

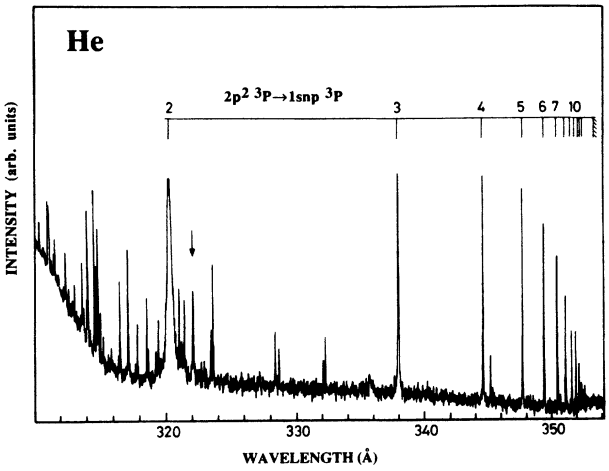

FIG. 2. Photometer recording of a part of a plate exposed 24 h to helium radiation showing the spectrum on the long-wavelength side of the He II α line. It exhibits the $2p^2\,^3P \rightarrow 1snp\,^3P$ Rydberg series between $n=2$ and $n=13$. The transition corresponding to $n=2$ is shown also in Fig. 4. Other parts of this recording are shown in Figs. 3 4, and 5. The arrow at 322 Å points out the broadened line reflecting the $2s2p\,^3P \rightarrow 1s2s\,^3S$ transition. A detailed recording of this line is shown in Fig. 6.

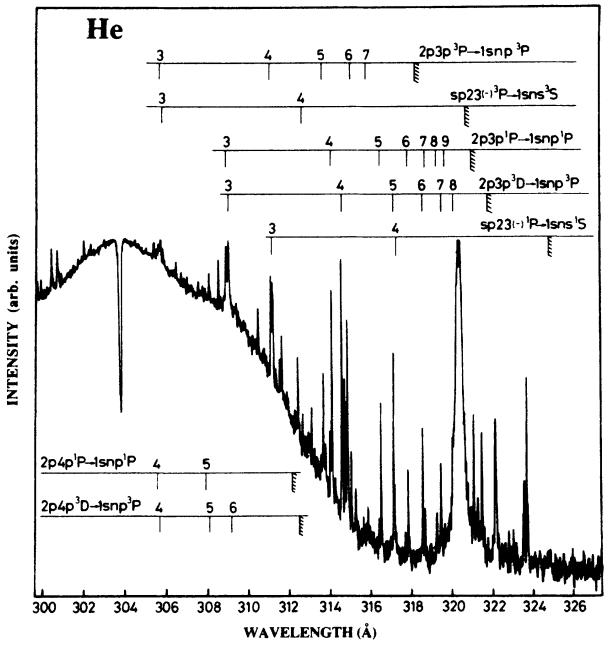

FIG. 3. Detail of the He spectrum showing the $2p^2\,^3P \rightarrow 1s2p\,^3P$ line (saturated in this spectrum) and superimposed on the high background of the He II α line a number of CIS (constant-initial-state) series arising from $2p3p$ and $2p4p$ initial states. Their apparent intensities are very low, particularly in the neighborhood of the background maximum. The first lines of these series are shown in Fig. 4.

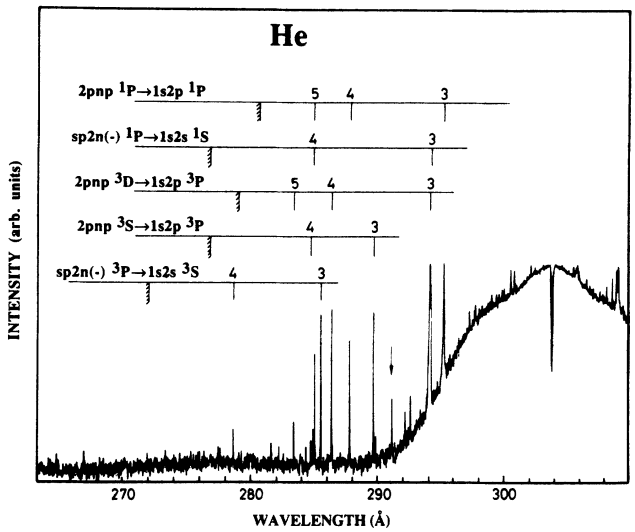

FIG. 4. Detail of the He spectrum showing the He II α line (strongly saturated) and a number of lines superimposed on the background at its high-energy side. Most of the lines correspond to CFS (constant-final-state) series involving $2pnp$ initial states. The lines due to the $2p3p\,^3D$ and ^1P states are strongly saturated. The arrow points at the line of the $2p3p\,^3P \rightarrow 1s2p\,^3P$ transition which is very weak (see text). Higher components of the CFS series have not been identified while the CIS series shows rather strong lines (cf. Fig. 3).

Fig. 4) is a grating ghost (31/40×303.78 Å) corresponding to the He II α radiation. Another weak line (not shown) appearing at 262.95 Å is probably a grating ghost arising from the He I α line (9/20×584.33 Å). Weak impurity lines are observed at 320.98 Å (due to O III) and at 323.5 Å (due to N III).

All assignments are made in terms of single

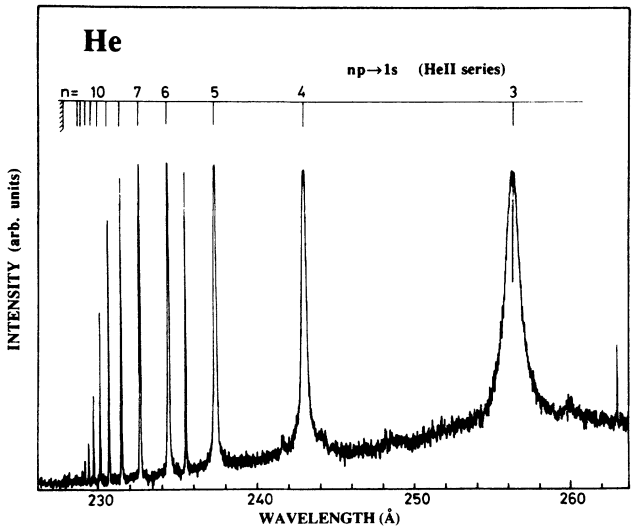

FIG. 5. Detail of the He spectrum showing the Lyman series $np \rightarrow 1s$ of He II between $n=3$ and $n=14$. All lines in the range up to $n=7$ are saturated in the spectrum. The line at 235.5 Å is due to a ghost reflection in the grating from the He I α line at 584 Å.

TABLE I. Observed transitions of He I. Theoretical results obtained by *ab initio* calculations of the upper state are also included (Refs. 7 and 8).

Observed wavelength (Å)	Relative intensity	Interpretation	Previous results (Å)	Theory (Å)
278.58	1	$sp24(-)\,^3P \rightarrow 1s2s\,^3S$		278.55
281.5	1			
283.37	3	$2p5p\,^3D \rightarrow 1s2p\,^3P$		283.33
284.68	1.5	$2p4p\,^3S \rightarrow 1s2p\,^3P$		284.65
284.85	1.5	$2p5p\,^1P \rightarrow 1s2p\,^1P$		284.85
284.88	1	$sp24(-)\,^1P \rightarrow 1s2s\,^1S$		284.85
284.99	7			
285.50	12	$sp23(-)\,^3P \rightarrow 1s2s\,^3S$	285[a]	285.40
286.33	12	$2p4p\,^3D \rightarrow 1s2p\,^3P$	286.4[b]	286.27
287.71	8	$2p4p\,^1P \rightarrow 1s2p\,^1P$		287.70
289.61	12	$2p3p\,^3S \rightarrow 1s2p\,^3P$		289.54
291.11	3	$2p3p\,^3P \rightarrow 1s2p\,^3P$		290.91
294.11	900	$2p3p\,^3D \rightarrow 1s2p\,^3P$	294.1[b]	294.00
294.20	20	$sp23(-)\,^1P \rightarrow 1s2s\,^1S$	293.8[a,c]	294.11
295.22	400	$2p3p\,^1P \rightarrow 1s2p\,^1P$	295.2[a,b]	295.13
300.49	80	$2p4p\,^3D \rightarrow 1s3p\,^3P$	300.6[b]	300.45
300.75	60	$2p4p\,^1P \rightarrow 1s3p\,^1P$		300.73
300.81	14			
302.09	300	$2p3d\,^3P \rightarrow 1s3d\,^1D$		302.02
302.43	200	$2p3d\,^3P \rightarrow 1s3d\,^3D$		302.36
305.46	400	$2p3d\,^1D \rightarrow 1s3d\,^1D$	305.2[b]	305.39
305.60	100	$2p4p\,^1P \rightarrow 1s4p\,^1P$		305.58
305.68	250	$2p4p\,^3P \rightarrow 1s4p\,^3P$	305.7[b]	305.64
305.76	1400	$2p3p\,^3P \rightarrow 1s3p\,^3P$	305.2[b]	305.55
305.89	80	$sp23(-)\,^3P \rightarrow 1s3s\,^3S$		305.80
307.93	40	$2p4p\,^1P \rightarrow 1s5p\,^1P$		307.93
308.13	30	$2p4p\,^3D \rightarrow 1s5p\,^3P$		308.07
308.96	300	$2p3p\,^1P \rightarrow 1s3p\,^1P$	309.1[b]	308.87
309.09	900	$2p3p\,^3D \rightarrow 1s3p\,^3P$	309.1[b]	308.97
310.24	20	$2p4p\,^3D \rightarrow 1s7p\,^3P$		310.20
311.15	40	$2p3p\,^3P \rightarrow 1s4p\,^3P$	311.1[b]	310.92
311.22	40	$sp23(-)\,^1P \rightarrow 1s3s\,^1S$	311.0[a]	311.12
312.64	10	$sp23(-)\,^3P \rightarrow 1s4s\,^3S$		312.55
313.68	8	$2p3p\,^3P \rightarrow 1s5p\,^3P$		313.44
314.09	15	$2p3p\,^1P \rightarrow 1s4p\,^1P$		313.99
314.59	35	$2p3p\,^3D \rightarrow 1s4p\,^3P$	314.6[b]	314.46
315.05	4	$2p3p\,^3P \rightarrow 1s6p\,^3P$		314.82
315.88	2	$2p3p\,^3P \rightarrow 1s7p\,^3P$		315.64
316.53	7	$2p3p\,^1P \rightarrow 1s5p\,^1P$		316.43
317.16	10	$2p3p\,^3D \rightarrow 1s5p\,^3P$		317.04
317.21	3	$sp23(-)\,^1P \rightarrow 1s4s\,^1S$		317.11
317.87	4	$2p3p\,^1P \rightarrow 1s6p\,^1P$		317.77
318.57	5	$2p3p\,^3D \rightarrow 1s6p\,^3P$		318.44
318.68	2	$2p3p\,^1P \rightarrow 1s7p\,^1P$		318.58
319.21	1.5	$2p3p\,^1P \rightarrow 1s8p\,^1P$		319.11
319.42	3	$2p3p\,^3D \rightarrow 1s7p\,^3P$		319.29
319.97	1	$2p3p\,^3D \rightarrow 1s8p\,^3P$		319.84
320.2925	3000	$2p^2\,^3P \rightarrow 1s2p\,^3P$	320.2925[d]	319.50
322.10	4	$2s2p\,^3P \rightarrow 1s2s\,^3S$		321.61
338.14	100	$2p^2\,^3P \rightarrow 1s3p\,^3P$	338.1[b]	
344.73	17.5	$2p^2\,^3P \rightarrow 1s4p\,^3P$	344.7[b]	
347.83	15.0	$2p^2\,^3P \rightarrow 1s5p\,^3P$		
349.52	12.7	$2p^2\,^3P \rightarrow 1s6p\,^3P$		
350.54	9.1	$2p^2\,^3P \rightarrow 1s7p\,^3P$		
351.20	5.9	$2p^2\,^3P \rightarrow 1s8p\,^3P$		
351.66	3.6	$2p^2\,^3P \rightarrow 1s9p\,^3P$		
351.99	3.1	$2p^2\,^3P \rightarrow 1s10p\,^3P$		

TABLE I. (*Continued*).

Observed wavelength (Å)	Relative intensity	Interpretation	Previous results (Å)	Theory (Å)
352.23	2.0	$2p^2\,{}^3P \rightarrow 1s11p\,{}^3P$		
352.41	1.3	$2p^2\,{}^3P \rightarrow 1s12p\,{}^3P$		
352.55	1.1	$2p^2\,{}^3P \rightarrow 1s13p\,{}^3P$		

[a] Reference. 10.
[b] Reference 2.
[c] Reference 11.
[d] Reference 12. The value is used as a wavelength standard in this study.

configurations. This is done merely to provide a simple means of identification whereas a proper description of the electronic properties usually requires inclusion of configuration interaction. Most of the spectral series in He I which have been identified can be characterized as either constant-initial-state (CIS) series or constant-final-state (CFS) series. The former involves a given doubly excited initial state and a series of singly excited final states whereas the latter involves a series of doubly excited initial states and a single singly excited final state. The former are of course more readily identified in the spectrum since the singly excited energy levels are in general very well known. Our assignments of the latter rely in part on earlier experimental data and also on theoretical results both regarding energies and effective principal quantum numbers of the Rydberg series. In the spectrum the CIS series converge towards a long-wavelength limit whereas the CFS series converge against shorter wavelengths.

In addition to the series observed, some single transitions of comparatively low intensity can be identified. Also, since the resolution of this study is comparatively high the details of many previously unresolved structures have been revealed. We present these in the last section. The strong lines in the spectrum from He I are observed essentially to correspond to transitions from the lowest levels of the doubly excited $nln'l'$ configurations, while the higher levels of each series give rise to lower and progressively decreasing intensity as expected. This agrees with observations for beam-foil spectra.[10] Furthermore, the configurational one-electron transitions are in most cases much stronger than those described as two-electron transitions. We include the relative peak height above the general background for each line in Table I. For lines appearing near the He II α line the relative height has been determined from a series of recordings using different exposure times. By this means the background influence on each line has been reduced to a minimum. Corrections have not been made for nonlinearities of the photographic plates (both regarding intensity and wavelength response). However, the strongest lines have been measured by means of a channel multiplier which suggests that the intensity response is approximately linear at intermediate photographic plate exposure densities. The lines which could be investigated in this manner have the following wavelengths in Å: 294.11, 295.22, 302.09, 302.43, 305.46, 305.68, 305.76, 308.96, 309.09, 320.29. Such studies could not be performed for the weaker lines because the signal-to-background ratio was too low.

A. CIS series

1. $2p^2 \rightarrow 1snp$ transitions

The $2p^2$ configuration gives rise to the three states ${}^1S$, ${}^3P$, and ${}^1D$, with even parity. In principle, three different series could thus appear in the spectrum. Of these only the ${}^3P$ series is strongly excited. It starts with a very intense line at 320.29 Å corresponding to the single electron transition $2p^2 \rightarrow 1s2p$ and can be followed up to $n = 13$. The data from this series shown in Figs. 3 and 4 are collected in Table I. The wavelength of this $2p^2 \rightarrow 1s2p$ transition has been accurately determined previously[12] and is used as a calibration standard in the present study as was mentioned above.

The transitions from the singlet states ${}^1S$ and ${}^1D$ to the $1s2p\,{}^1P^o$ final state are expected to appear at 319.80 Å (${}^1D$) and 302.99 Å (${}^1S$), respectively.[1] There is a weak line at 319.87 Å superimposed on the tail of the ${}^3P \rightarrow {}^3P$ line at 320.2 Å which energetically fits to the former transition. However, the autoionization width of the ${}^1D$ state has been calculated to be extremely large,[7] in contrast to the observed linewidth, so this assignment must be excluded. The predicted lifetime of the ${}^1S$ state is, on the other hand, so large that transitions from this state could give rise to a well-defined line. No line has been observed at the expected wavelength but this can be due to the high background level at this position.

2. $2p3p \rightarrow 1snp$ transitions

The $2p3p$ initial-state electron configuration gives rise to six states ${}^{1,3}S$, ${}^{1,3}P$, and ${}^{1,3}D$. For three of these (${}^3S$, ${}^1P$, and ${}^3D$) the $2p3p$ configuration is the lowest possible with respect to the principal quantum number whereas for the other three states the $2p^2$ configuration is lowest. The former states give rise to series of substantial intensity. This is easily observed for the ${}^1P$ ($2p3p\,{}^1P^e \rightarrow 1snp\,{}^1P^o$) and ${}^3D$ ($2p3p\,{}^3D^e \rightarrow 1snp\,{}^3P^o$) states (Figs. 3 and 4) which both give rise to long series, the former starting at 295.22 Å and the latter at 294.11 Å with very strong lines. The

calculated autoionization rate of the triplet state is very low,[7,13–15] which partly explains the high intensity of the transition. In one of the earlier beam-foil studies the 294.11-Å line was found to have the wavelength 293.8 Å and was then associated with the $sp23(-)\,^1P \rightarrow 1s2p\,^1P$ transition. As is discussed below this transition does occur in the same wavelength region but the intensity is found to be an order of magnitude smaller than for that from the $2p3p\,^3D$ and also the $2p3p\,^1P$ state. The data are included in Table I.

The series arising from the $^3S^e$ initial state, that is, $2p3p\,^3S \rightarrow 1snp\,^3P$, on the other hand, is expected, with the exception of the first component, to fall at the He II α line and cannot therefore be observed. The first component ($n=2$) is expected to occur between 289 and 290 Å where the background is low. The energy value of the ^3S state given in Ref. 1, 63.81 eV, is probably not very accurate so the theoretical value of 63.786 eV should be more reliable in this case. This gives a wavelength for the transition of 289.54 Å which is in close agreement with a sharp line in our spectrum at 289.61 Å. Since the autoionization width of this ^3S state is predicted to be very small, this assignment seems well justified.[7] For the surrounding peaks of similar intensity in the spectrum (cf. Fig. 4) higher components of the corresponding expected CFS series can be observed at shorter wavelengths (cf. Sec. III B). One could therefore expect to find also a peak corresponding to the $2p4p\,^3S \rightarrow 1s2p\,^3P$ transition. From the calculated data a wavelength of 284.65 Å is obtained which fits excellently with a weak peak observed at 284.68 Å.

No transitions have been observed corresponding to the ^1S and ^1D initial states. This parallels the result for the $2p^2$ configuration but again the ^1S state would have a lifetime sufficient to give rise to a spectral line. The $2p3p\,^3P \rightarrow 1s2p\,^3P$ transition which is expected to appear at 291 Å has been predicted to have very low transition probability[16] and has not been detected in earlier studies by the beam-foil technique. In our spectrum the line is observed at 291.11 Å with very low intensity (Fig. 4). Starting at this wavelength a series of lines can be followed in close agreement with expected wavelengths for a $2p3p\,^3P \rightarrow 1snp\,^3P$ series up to $n=7$. As can be seen the relative intensity is much higher for the transitions to the $1s3p$ and $1s4p$ states. At least the former can be qualitatively rationalized in terms of a one-electron picture.

3. *2p4p→1snp transitions*

The two strong series emanating from the $2p3p\,^1P$ and ^3D initial states are accompanied by weaker series associated with the initial $2p4p\,^1P$ and ^3D states (Figs. 3 and 4). For the latter state a fairly well determined energy exists[1] [64.254(12) eV] and based on that value the series can be readily identified in our spectrum. From the most well-defined peaks of our spectrum a more accurate value for this ^3P state can be obtained. This is 64.267(2) eV. For the former state (^1D) no experimental value has been given earlier. However, a calculated value exists[7] which suggests that the first component of the expected series is to be found at 287.68 Å. This is in good agreement with our spectrum which gives the value 287.71 Å. Furthermore, several higher components which may be associated with such a series are observed in support of the assignment. From these data and energies of singly excited states of Ref. 1 the energy of the $2p4p\,^1P$ state is obtained as 64.312(2) eV.

4. *sp23(−)→1sns transitions*

The $sp23(-)$ initial-state electron configuration gives rise to the two $^{1,3}P^o$ states. Theoretical studies suggest that the autoionization rate is low for both states[7,15] and earlier experimental evidence has been found for their presence in radiative transitions.[10,12] It is generally agreed that the $sp23(-)\,^1P \rightarrow 1s2s\,^1S$ transition occurs at about 294 Å. In this region of the spectrum (Fig. 4) only a single line remains to be assigned. It has a wavelength of 294.20 Å. Starting at this point one can furthermore infer an accompanying short CIS series with energy spacings of the $1sns$ series.[1] Hence we get a value of 62.759 eV for the $sp23(-)\,^1P$ state in close agreement with 62.758(10) eV given earlier.[1]

The $sp23(-)\,^3P \rightarrow 1s2s\,^3S$ transition is expected to appear at 285.5 Å.[12] We associate this transition with the line at 285.50 Å (Fig. 4) to which a short series can be attached with the expected energy spacings for the $1sns\,^3S$ series.[1] This leads to an energy of 63.247 eV for the $sp23(-)\,^3P$ state in support of the tentative assignment given in Ref. 1 and in rather close agreement with the value given in Ref. 10 (63.244 eV).

B. CFS series

1. *np→1s series in He II*

This is the most obvious series of the spectrum starting with the He II α line at 303.78 Å corresponding to the $2p \rightarrow 1s$ transition. Figure 5 shows the higher components ranging from $3p \rightarrow 1s$ to $14p \rightarrow 1s$. Where comparisons can be made (for $np \rightarrow 1s$; $n \leq 12$) good agreement is found between our results and the data reported earlier.[1]

The energy range containing this He II series was recently studied by means of beam-foil technique.[6] In particular, a number of weak structures surrounding the lines of the He II series were associated with transitions in doubly excited He I. These structures are not present in our spectrum (Fig. 5), although many of the lines of the He II series have extremely high intensity relative to the background and despite the fact that doubly excited states are efficiently populated in our uv source.

2. *2pnp $^3D \rightarrow 1s2p\,^3P^o$ series*

The $n=3$ and $n=4$ components have been identified in Sec. III A. One more line of this series corresponding to $n=5$ can be inferred from the spectrum. The energy agrees well with that obtained in the *ab initio* calculations of Ref. 8. Another quantity which can be used for comparison is the effective quantum number n^* referred to the outer electron. It has been found that when using the following simple formula for the energy levels the

TABLE II. Energy and effective principal quantum number n^* for doubly excited states of He I. The error limits in the energy values of the present study are 0.002 eV. Previous energies are obtained from Ref. 1 and theoretical values from Ref. 7.

Assignment	Energy (eV) This study	Energy (eV) Previous studies	Quantum no. n^* This study	Quantum no. n^* Theory
$2p^2\,^3P$	59.6744	59.6744	1.542	1.555
$2p3p\,^3P$	63.555	63.555(6)	2.710	2.738
$sp23(-)\,^1P$	62.759	62.758(10)	2.270	2.276
$sp24(-)\,^1P$	64.141	64.141(16)	3.287	3.290
$sp25(-)\,^1P$	64.661	64.67(2)	4.289	4.293
$2p3p\,^3D$	63.120	63.120(6)	2.443	2.452
$2p4p\,^3D$	64.267	64.254(12)	3.463	3.476
$2p5p\,^3D$	64.718		4.466	4.485
$2p3p\,^1P$	63.216	63.219(15)	2.496	2.503
$2p4p\,^1P$	64.312		3.536	3.544
$2p5p\,^1P$	64.745		4.556	4.559
$sp23(-)\,^3P$	63.247	63.246(3)	2.514	2.523
$sp24(-)\,^3P$	64.326		3.559	3.566
$2p3d\,^1D$	63.664	63.673(12)	2.799	2.807
$2p3p\,^3S$	63.775	63.81	2.894	2.904
$2p4p\,^3S$	64.517		3.925	3.935
$2p3d\,^3P$	64.070	64.0726(10)	3.199	3.210
$2p3d\,^1P$	64.117	64.16	3.256	3.268

effective quantum number differs only slightly between different members of a given series,

$$E=-\frac{1}{2}\left[\left[\frac{Z}{N}\right]^2+\left[\frac{Z-1}{n^*}\right]^2\right]. \quad (1)$$

N is the principal quantum number of the inner electron. The energy is obtained in a.u. Invoking our measured energies the values calculated for n^* by this formula are almost the same for the different levels and also compares very well with the calculated data[7,8] which support the assignments. The results are summarized in Tables I and II.

3. $2pnp\,^3S \rightarrow 1s2p\,^3P$ series

Since the ^3S state is much higher in energy than the ^3D state this series starts at shorter wavelengths. As was discussed above we associate this transition with the line at 289.61 Å and the second component ($n=4$) with the weak line at 284.68 Å. The energy spacing between the lines in the spectrum is unusually small due to the high value of the effective quantum number n^* (cf. Table II). The higher components are too weak to be clearly separated from the background in this study.

4. $2pnp\,^1P \rightarrow 1s2p\,^1P$ series

The components with $n=3$ and $n=4$ were identified in Sec. III A. As in the case of the ^3D series, an additional line corresponding to $n=5$ can be identified. A comparison with calculated data[7,8] shows very good agreement regarding both the energies and the effective quantum number n^* obtained from Eq. (1). The data are collected in Tables I and II.

5. $sp2n(-)\,^1P \rightarrow 1s2s\,^1S$ series

The first component ($n=3$) was identified in the above as corresponding to the line at 294.20 Å (cf. Table I). Using energy values from Ref. 8 the expected wavelengths for higher components can be calculated. For the first of these ($n=4$) a wavelength of 284.85 Å is obtained exactly the same as for the $2p5p\,^1P \rightarrow 1s2p\,^1P$ transition. However, it is likely that the experimental wavelength is somewhat larger as for the $n=3$ transition. In fact, the peak with maximum intensity at 284.85 Å has a shoulder centered approximately at 284.88 Å and we tentatively associate this structure with the $n=4$ transition. The next component with $n=5$ is expected to appear at 281.49 Å according to the calculation of Ref. 8. It probably contributes to the weak line at 281.5 Å.

6. $sp2n(-)\,^3P \rightarrow 1s2s\,^3S$ series

As was discussed above, this series starts at a short wavelength and the first line is comparatively weak (cf. Table I). Energy values for the higher components have been predicted theoretically.[7,8] The second one (corresponding to $n=4$) is expected to appear at 278.55 Å. This is in very good agreement with the single weak line observed in this region of the spectrum. Additional transitions of this series are probably too weak to be observed in the present investigation.

C. Special details of the spectrum

1. $2s2p\,^3P \rightarrow 1s2s^3S$ transition

The $2s2p\,^3P^o$ state is the lowest in the $nsn'p\,^3P$ manifold of double excitations. Transitions to the ^3S final state, which can be described in a one-electron picture,

would therefore be highly likely provided that autoionization is not too fast. Earlier studies in the optical region show that substantial photon emission does occur and suggest that autoionization in the initial state gives rise to a line broadening of the order of 7 meV (Ref. 5) which would be substantial at our spectrometer resolution. We observe the line at 322.10 Å exactly where it is expected to appear.[1] As can be seen in the figure, the line is broadened. To show this more clearly a detailed recording of the line is given in Fig. 6 together with a nonbroadened line exhibiting the spectrometer width. These recordings are obtained from photographic plates giving nonlinear intensity scale so the linewidth is not possible to determine accurately. A lifetime broadening of 7 meV is, however, consistent with our result. It can be noted that the broadening of the line is entirely due to the short lifetime of the initial state since the final state is metastable.

2. *Lines between 311 and 309 Å*

At 311 Å a single line has been observed in previous studies.[2,12] In Ref. 2 it was assigned as the $2p3p\ ^3P \rightarrow 1s4p\ ^3P$ transition and in Ref. 12 as the $sp23(-)\ ^1P \rightarrow 1s3s\ ^1S$ transition. In our spectrum, in fact, two lines are resolved with approximately the same magnitude (cf. Fig. 7). The wavelengths fit very well into the Rydberg series involving these two transitions (cf. Table I) so the assignments are straightforward.

Also at 309 Å two lines are resolved (cf. Fig. 8) whereas only one line has been observed in earlier studies.[2,12] Two different assignments have been suggested, one in the singlet and one in the triplet system. Both correspond to members of strong Rydberg series and obviously give rise to the two lines observed (cf. Table I). In Ref. 2 it was argued on the bases of autoionization rates that the $^1P \rightarrow {}^1P$ transition is likely to be the more dominating. As can be seen from our spectrum the opposite is true although the intensities are of similar magnitude.

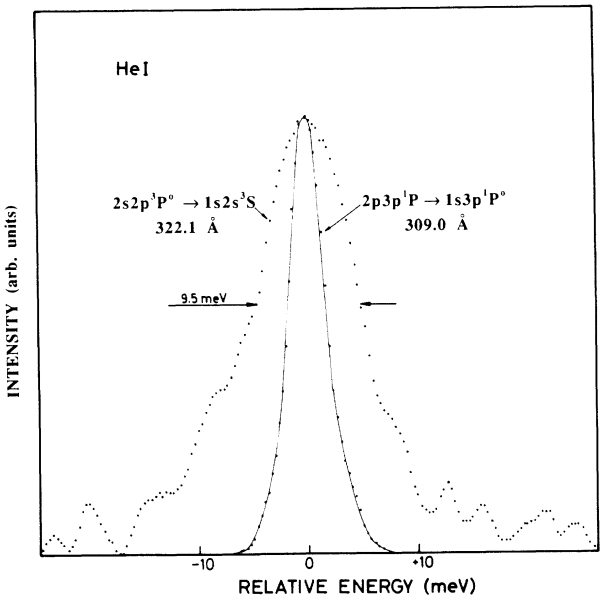

FIG. 6. Digitized data from photometer recordings of the two lines at 322.0 Å and 309.1 Å drawn with the peak maxima at the same position. The first line corresponding to the $2s2p\ ^3P \rightarrow 1s2s\ ^3S$ transition is substantially broadened by autoionization of the initial state whereas the latter line is considered to show essentially the spectrometer broadening. The periodic background intensity variations of the 322.0-Å line are primarily due to the grain size of the photographic plate. The exposure time of the plate was 24 h.

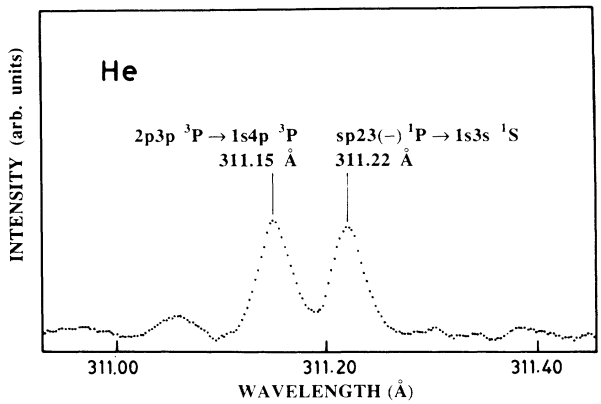

FIG. 7. Detailed recording showing the two close-lying lines at 311 Å. The exposure time was 5 h.

3. *Structures at 305 Å*

Earlier studies by means of beam-foil spectroscopy have revealed first a single line at 306 Å (Ref. 10) and later two lines at 305.7 and 305.2 Å.[2] At the higher resolution used in our study five lines can be observed as shown in Fig. 9. The four lines with the longest wavelengths can all be associated with Rydberg series and correspond to one-electron transitions. The line at 305.46 Å cannot be fitted into a Rydberg or sequence series in the same manner which suggests that the transition involves

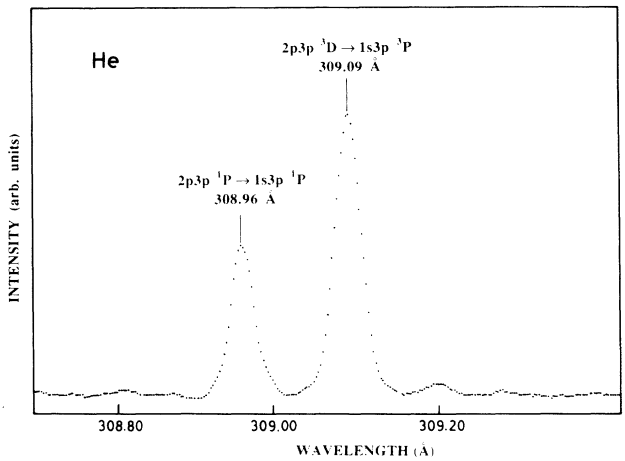

FIG. 8. Detailed recording of the two intensive lines at 309 Å. The lines are strongly saturated in the spectrum of Fig. 4 and saturation effects can be observed also in this spectrum. The exposure time of the plate was 1 h.

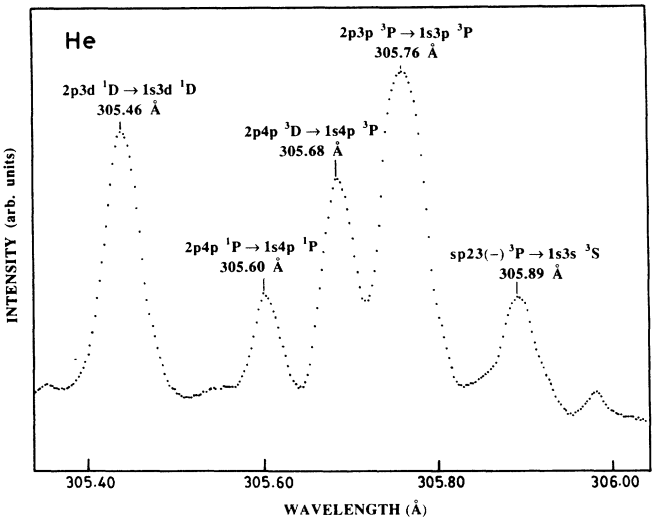

FIG. 9. Detailed recording of the structures observed at 305 Å. Some of the lines are strongly saturated. The exposure time of the plate was 1 h.

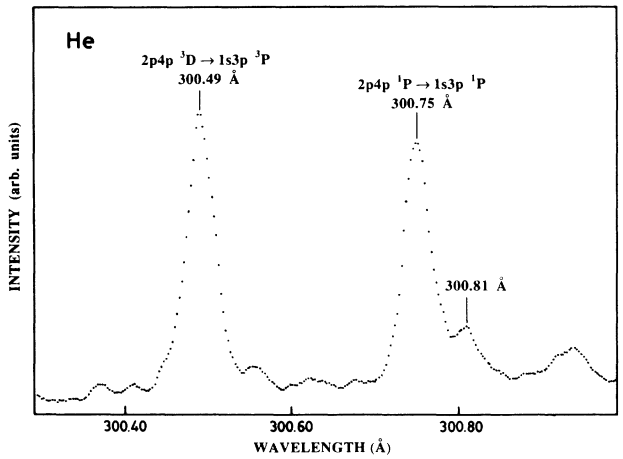

FIG. 11. Detailed recording at 300 Å. In the overall spectrum of Fig. 4 one observes only some weak features superimposed on the high background of the He II α line. The exposure time of the plate was 1 h.

some d-type orbital. Such transitions tend to give lines close to the He II α line and the Rydberg series for those are therefore difficult to observe. Calculations[8,17] suggest that the $2p3d\ ^1D \rightarrow 1s3d\ ^1D$ transition should have almost exactly the wavelength we observe and this assignment was also proposed for the structure observed previously at 305.2(2) Å (Ref. 2). It thus seems most likely that the line at 305.46 Å corresponds to this transition. This assignment leads to an energy of 63.664 eV for the $2p3d\ ^1D$ state with a value of n^* equal to 2.799 in very good agreement with the theoretical value. The data are included in Table II. The relative intensities of the lines are very different, the line at 305.76 Å being strongly dominating.

4. *Lines around 302–300 Å*

In this wavelength region a number of lines are present. Many of them probably involve some of the

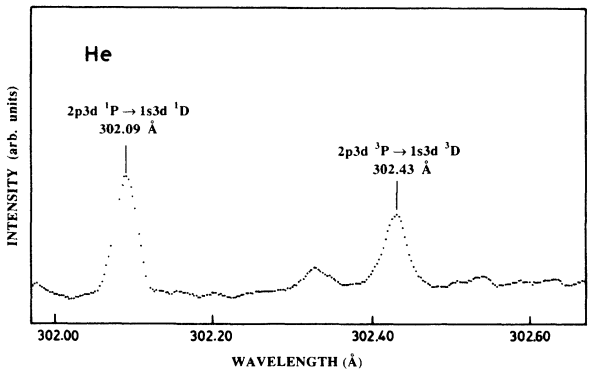

FIG. 10. Detailed recording at 302 Å showing transitions which involve d orbitals. The exposure time of the plates was 1 h.

$npn'd$ electron configurations which tend to give transitions in the range of the He II α line. Due to the high background from the He II α line the apparent intensity of many of these lines is very low so it is difficult to identify any Rydberg series. However, the line at 302.43 Å (cf. Fig. 10) is most probably due to the $2p3d\ ^3P \rightarrow 1s3d\ ^3D$ transition which is expected to have high intensity. In this assignment the energy of the $2p3d\ ^3P$ state is found to be 64.070 eV in very good agreement with a previously determined value[1] and the calculated value.[8] These results are given in Table II.

It is reasonable to assume that also the line at 302.09 Å involves a d type orbital and in particular a $2p3d$ initial state. Both the ^1D and ^3D states lead to emission on the long wavelength side of the He II α line so they can be excluded. For the $2p3d\ ^1P$ state only an approximate value of 64.16 eV is given in Ref. 1 and the result of the *ab initio* calculation[7,8] is much lower, 64.126 eV. Since the calculations have proved to be accurate in all other cases where comparisons are possible we base the interpretation mainly on this value. The transition to be considered is $2p3d\ ^1P \rightarrow 1s3d\ ^1D$. Using our measured value of 302.09 Å we obtain the energy 64.117 for the initial state which is in good agreement with the calculation. Since the $2p3d\ ^1P$ state is not substantially broadened by autoionization[7] we find this assignment well justified.

Figure 11 shows the region around 300 Å exhibiting two components of the series arising from the $2p4p$ initial-state configuration. The origin of the weaker line at 300.81 Å is unknown.

ACKNOWLEDGMENT

Dr. Reinhold Hallin is gratefully acknowledged for pointing out the existence of emission lines in doubly excited He to us.

[1]W. C. Martin, J. Phys. Chem. Ref. Data **2**, 257 (1973).
[2]E. J. Knystautas and R. Drouin, Nucl. Instrum. Methods **110**, 95 (1973).
[3]K. Ishii and M. Tomita, J. Phys. Soc. Jpn. **45**, 230 (1978).
[4]R. L. Brooks and E. H. Pinnington, Phys. Rev. A **22**, 529 (1980).
[5]H. Cederquist, M. Kisielinski, and S. Mannervik, J. Phys. B **16**, L479 (1983).
[6]R. Bruch, P. L. Altick, E. Träbert, and P. H. Heckmann, J. Phys. B **17**, L655 (1984).
[7]M. J. Conneely and L. Lipsky, J. Phys. B **11**, 4135 (1978).
[8]L. Lipsky, R. Anania, and M. J. Conneely, At. Data Nucl. Data Tables **20**, 127 (1977).
[9]P. Baltzer (unpublished).
[10]H. G. Berry, I. Martinson, L. J. Curtis and L. Lundin, Phys. Rev. A **3**, 1934 (1971).
[11]H. G. Berry, J. Desequelles, and M. Dufay, Phys. Rev. A **6**, 600 (1972).
[12]J. L. Tech and J. F. Ward, Phys. Rev. Lett. **27**, 367 (1971).
[13]J. W. Cooper, S. Ormonde, C. H. Humphrey, and P. G. Burke, Proc. R. Soc. London **91**, 285 (1967).
[14]P. L. Altick and E. N. Moore, Proc. R. Soc. London **92**, 853 (1967).
[15]J. W. Cooper, U. Fano, and F. Prats, Phys. Rev. Lett. **10**, 518 (1963).
[16]G. W. F. Drake, Phys. Rev. A **5**, 614 (1972).
[17]H. Doyle, M. Oppenheimer, and G. W. F. Drake, Phys. Rev. A **5**, 26 (1972).